Journal of Cellular Biochemistry 75:578–586 (1999)

Changes of Chromatin Condensation in One Patient With Ataxia Telangiectasia Disorder: A Structural Study

Laura Vergani,[1]* **Giuseppina Fugazza,**[1] **Luciana Chessa,**[2] **and Claudio Nicolini**[1]

[1]Institute of Biophysics, School of Medicine, University of Genoa, 16132 Italy
[2]Department of Experimental Medicine and Pathology, University of Rome "La Sapienza," Rome, Italy

Abstract Differential scanning calorimetry and quantitative fluorescence microscopy have been employed to characterize the structure and organization of in situ chromatin in lymphoblastoid cells obtained from one ataxia telangiectasia (A-T) patient and one healthy family member. The proven capability of these biophysical techniques to measure changes of chromatin condensation directly inside the cells makes them very powerful in studying the eventual structural changes associated with the appearance of a pleiotropic genetic disorder such as ataxia telangiectasia. A-T syndrome is genetically heterogeneous and can be induced by different mutations of a single gene. The aim of this work is to determine whether the genetic mutation exhibited by the A-T patient of this study may be associated with modifications of chromatin structure and organization. Both the calorimetric and the fluorescence microscopy results acquired on cells from the A-T patient show that the structure and distribution of nuclear chromatin in situ change considerably with respect to the control. A significant decondensation of the nuclear chromatin is in fact associated with the appearance of the A-T disorder in the A-T patient under analysis, together with a rearrangement of the chromatin domains inside the nucleus. J. Cell. Biochem. 75:578–586, 1999.

Key words: ataxia telangiectasia disorder; chromatin structure; differential scanning calorimetry; quantitative fluorescence microscopy

Ataxia telangiectasia (A-T) is an autosomal recessive disorder characterized by cerebellar degeneration, immunodeficiency, chromosomal instability, cancer predisposition (particularly to leukemias and lymphomas), radiation sensitivity, and cell cycle abnormalities [for a review see Lavin and Shiloh, 1997]. People with A-T usually die in their teens or early 20s [Savitsky et al., 1995; Brown et al. 1997; Fitzgerald et al., 1997]. A-T carriers exhibit an increased sensitivity to X-rays and an increased risk of cancer [Bishop et al., 1997].

The pleiotropic nature of the A-T disorder is also manifested in the cellular phenotype. Cells of A-T patients have a reduced life-span, defects in cytoskeleton, increased sensitivity to ionizing radiation, and defects in the checkpoints at the G1 and G2 phase of the cell cycle [Savitsky et al., 1995, 1997].

Grant sponsor: University of Genoa, 1997 and 1998.

*Correspondence to: Laura Vergani, Institute of Biophysics, School of Medicine, Corso Europa 30, 16132 Genoa, Italy. E-mail: vergani@ibf.unige.it

Received 12 February 1999; Accepted 13 May 1999

In the last few years the A-T disorder has proved to be genetically heterogeneous, depending on different mutations of a single gene localized on chromosome 11. The A-T gene (ATM) has been recently identified [Savitsky et al., 1995] and it is probably involved in cell cycle control [Brown et al., 1997].

According to the ever more accepted hypothesis of a central role of chromatin structure in regulating the gene expression [for a review see Nicolini, 1997], the observed differences of cellular phenotype between cells isolated from the A-T patients and the healthy control may be related to modifications of the condensation and spatial distrtibution of interphase chromatin.

It is well known that inside the interphase nucleus the eukaryotic chromatin exhibits different levels of condensation which could be correlated with the transcriptional activity [Lamond and Earnshaw, 1998; Zink et al., 1998]. A well-accepted hypothesis suggests that highly condensed domains of nuclear chromatin can be in a transcriptionally inactive state, while less condensed regions are actively transcribed [Fenster et al., 1974; van Holde, 1989; Wolfe,

1994]. Actually, a recent paper [Ellis et al., 1996] shows that the relationship between chromatin condensation and transcriptional activity is more complicated.

Quantitative fluorescence microscopy is considered up to now to be one of the most powerful techniques in studying the nuclear chromatin in situ. It has been proved that the fluorescence intensity of nuclei stained with DNA-selective fluorochromes is related to both the DNA content and DNA-chromatin structure. The DNA accessibility is in fact strictly dependent on its condensation [Myc et al., 1992; Vergani et al., 1992; Nicolini et al., 1997; Vergani et al., 1998]. Therefore this technique allows us to extract from the nuclear images the topographical parameters related to the structure and organization of in situ chromatin [Belmont et al., 1994; Mascetti et al., 1996].

Complementary information about chromatin structure at the level of native cells or nuclei can also be obtained from differential scanning calorimetry. In fact it has been observed that the melting profile of chromatin exhibits different distinguishable thermal transitions [Nicolini et al., 1983, 1988; Touchette and Cole, 1985; Russo et al., 1995; Gavazzo et al., 1997; Vergani et al., 1997]. Each transition corresponds with the unfolding of an energetically characterized domain and it can be observed on both isolated and in situ chromatin fibers. It is interesting to note that the information obtained from the fluorescence microscopy is at the level of single cells, while the calorimetry supplies average data obtained on a cellular population (more than 10^9 cells for sample), therefore allowing greater statistical accuracy in the results. In this study we employed both of these techniques in order to evaluate the phenomena of folding/unfolding which occur in the nuclear chromatin as a function of the A-T disease.

MATERIALS AND METHODS

Cell Culture

The lymphoblastoid cell lines from the A-T patient (AT44RM) and his healthy relative (243RM) used as a control originated from the Cell Repository of the Italian Registry for Ataxia Telangiectasia [Chessa et al., 1994]. The cells were cultured in RPMI 1640 medium supplemented with fetal calf serum 15% and gentamycin 0.2%. The cultures were maintained at 37°C with 5% CO_2 atmosphere.

The mutation of the analyzed A-T patient is known: a deletion of 201 base pairs at the codon 1407 in exon 12 [Gilad et al., 1997].

Before the experiments the cells were synchronized at the G1/S phase of the cell cycle by incubation with Hydroxiurea 2 mM for 15 h.

For the calorimetric measurements native nuclei have been isolated in 0.5% NP-40 and washed twice in a hypotonic buffer (10 mM Tris-HCl pH 7.4, 10 mM NaCl, 3 mM $MgCl_2$). Before the calorimetric measurements the nuclear suspension was centrifuged at 8,000*g* for 30 min; then the pellet was loaded in the proper capsule.

Calorimetry

The wide use of differential scanning calorimetry (DSC) for structural analysis of intact cells and nuclei is due to its ability in measuring nonhomogeneous and very complex biological samples that cannot be observed using classical spectroscopy techniques.

DSC experiments were performed on a Perkin Elmer DSC-2 within the usual temperature range (310–410 K), at a scan rate of 5°/min, as previously described in detail [Nicolini et al., 1988]. Deconvolution of the heat capacity profiles into Gaussian components was carried out by least square fitting as already reported [Vergani et al., 1997]. At least three different measurements of each sample were acquired in order to check the accuracy and statistical significance of the experiment.

Fluorescence Microscopy

A Zeiss Axioplan light microscope (Zeiss, Oberoken, Germany) properly modified for computer controlled data acquisition was used as previously described [Mascetti et al., 1997]. For each sample the images of about 30 cells were acquired through Zeiss Plan-Neofluar objective lens: in particular we used a 100×/NA = 1.3 oil immersion lens (depth-of-field of 1.23 μm) and a 40×/NA = 0.75 lens (depth-of-field of 5.17 μm). The epifluorescence set-up consists of a 365 nm band pass excitation filter, a 395 dichroic mirror and a combination of a 397 nm long pass and 450–490 band pass emission filters. Digital pictures were obtained by an air-cooled (−40°C) scientific grade charge-coupled device (CCD) camera (Photometrics, Tucson, AZ) operating with a dynamic range of 12 bit (gray levels from 0 to 4,095) and excellent linearity and sensitivity.

In order to obtain quantitative information, shading correction and dark image subtraction have been applied to each image as previously described [Mascetti et al., 1996]. Before the calculations the out-of-focus contributions were removed from each 100× image by using the nearest-neighbor algorithm [Agard, 1984; Hiraoka et al., 1987]. Then the constrained deconvolution was applied to sharpen the image [Agard, 1989]. For each image the Integrated Fluorescence Intensity (IFI) was calculated as the summation of the intensity of each pixel within the projected nuclear image. This parameter represents a good estimation of the amount of dye contained in the corresponding nuclear slice. At low magnification the projected image corresponds to a nuclear slice of about 5 μm in thickness. Therefore in this case the integrated intensity represents a good estimation of the total amount of DAPI contained in a nucleus of about 5 μm in diameter (that is the just mean nuclear diameter). Consequently when, as in this study, we measure samples with the same amount of DNA, the Integrated Fluorescence Intensity is related to the average chromatin condensation exhibited by the nucleus. A linear relationship between the packing of nuclear chromatin and the dye uptake has in fact been demonstrated [Mascetti et al., submitted]. In order to obtain information about the distribution of DAPI inside the intact nucleus, after the proper correction for the out-of-focus contributions, we calculated the fluorescence histogram (pixel number versus gray level) of each 100× image. Therefore it is possible to distinguish among chromatin fibers with a different condensation on the basis of their relative fluorescence intensity inside the nucleus [Nicolini et al., 1997].

In order to quantitatively evaluate the topographical distribution of chromatin domains inside the nucleus we used three parameters [Young et al., 1986]. "Heterogeneity" parameter refers to the level of chromatin condensation. Therefore when the nucleus appears uniformly gray we obtain a value of 0, while a completely condensed nucleus will give us a value of 1. If the number of black pixels is N_B, the number of gray pixels is N_G, and the number of white pixels is N_W then we have: Hetero = $N_B + N_W/N_B + N_G + N_W$.

"Clump" provides information about the size of the chromatin granules: If a mesh of 0.5 m is used, the clump values will be 0 if all the granules are smaller than the mesh size, whereas it will be 1 if all the granules are larger than the mesh size.

"Condensation" reflects the fraction of large granules with respect to the total nuclear area.

RESULTS

When the temperature of native nuclei is increased at a constant rate, different peaks appear in the heat absorption profile. Each of these peaks has been associated with the melting of a specific molecular constituent. In physiological conditions isolated nuclei exhibit three distinguishable thermal transitions centered at about 342 K (I Transition), 359 K (II Transition), and 373 K (III Transition). As previously reported for different cellular systems [Nicolini et al., 1983, 1988; Touchette and Cole, 1985; Russo et al., 1995; Gavazzo et al., 1997; Vergani et al., 1997] these transitions have been assigned as follows: Transition I to nuclear proteins (residual cytoskeletal filaments, nuclear matrix, and histones), Transition II to nucleosome organized into a 10 nm filament (unfolded fiber), Transition III to nucleosome organized in highly folded fibers (30 nm or more). After the Gaussian decomposition, Transition II results in being constituted by two components centered at 356 and 362 K, which we referred to as II_a and II_b respectively. These components were previously assigned [Russo et al., 1995] to the melting of the two portions of the nucleosomal DNA in unfolded conformation: the linker and the core particle DNA, respectively. In addition, Transition III results in being constituted by two components centered at about 370 and 375 K, which we referred to as III_a and III_b, respectively. These transitions represent the melting of chromatin fibers with different degrees of condensation [Russo et al., 1995; Vergani et al., 1997].

The calorimetric profiles of nuclei isolated from the two cell lines under analysis (the A-T patient and the control, respectively) are reported in Figure 1. They exhibit a small but significant change in the enthalpy distribution. In particular (Table I) Transition II (corresponding to the melting of nucleosomal DNA), shows a rearrangement of the two components II_a and II_b with an increase of the enthalpy of transition II_a (from 0.299 to 0.343) and a similar decrease of the transition II_b (from 0.138 to

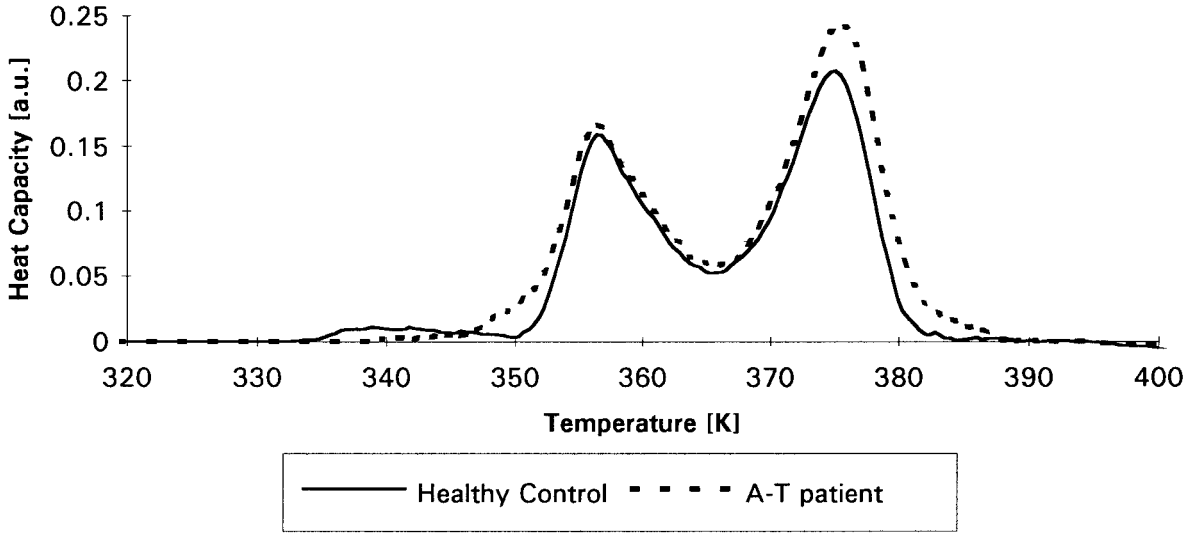

Fig. 1. Profiles of heat capacity (arbitrary units) vs. temperature (K) for nuclei isolated from the A-T patient (cell line AT44RM) and the healthy relative (cell line 243RM).

TABLE I. Relative Melting Enthalpy of the Main Thermal Transitions Exhibited by Nuclei Isolated From Cultured Lymphoblasts of One A-T Patient (Cell Line AT44RM) and His Healthy Family Member (Cell Line 243RM)

Thermal transitions					
Lymphoblasts	I 342 K	II_a 356 K	II_b 362 K	III_a 370 K	III_b 375 K
Healthy control	0.067 ± 0.015	0.299 ± 0.024	0.138 ± 0.030	0.121 ± 0.023	0.374 ± 0.018
A-T patient	0.024 ± 0.021	0.343 ± 0.028	0.107 ± 0.026	0.153 ± 0.014	0.374 ± 0.017

0.107). Therefore these changes suggest that in comparison with the control the A-T cells exhibit a partial unfolding of the core DNA which becomes detached from the histonic octamer, increasing in this way the portion of the linker DNA. The A-T patient also exhibits an increase in the enthalpy of transition III_a (from 0.121 to 0.153), the transition III_b remaining almost constant (0.374). This result can be explained by a partial unfolding of the highly condensed chromatin towards a partially folded fiber.

When the same samples are analyzed by fluorescence microscopy the nuclear images (Fig. 2) can provide complementary information about the chromatin condensation and the topographical distribution of its domains inside the nucleus. Table II reports the values of the Integrated Fluorescence Intensity for nuclei isolated both from the A-T patient and the control. It can be observed that the fluorescence intensity is higher in the A-T patient than in the control (fluorescence values of 3 and 3.8, respectively). Starting from previous published works, this increase of DAPI uptake can be interpreted as a decondensation of the nuclear chromatin in the A-T patient. In parallel we observe an increase in the nuclear area of cells from the A-T patient with respect to the healthy relative (15.2 vs. 27.3 m^2). This increase of area corresponds to a volume increase, both the nuclei under analysis being spherical. An inverse relationship between chromatin condensation and nuclear volume has been previously suggested by several groups [Nicolini et al., 1984; Haussinger, 1996; Vergani et al., 1998]. Therefore the increase of nuclear volume in the A-T patient cells is in accordance with the observations on the chromatin unfolding as a consequence of the A-T disorder.

When the nuclear images are acquired at a higher resolution, information about the chromatin texture and distribution inside the nucleus can be obtained by analyzing the fluorescence histograms calculated on the pro-

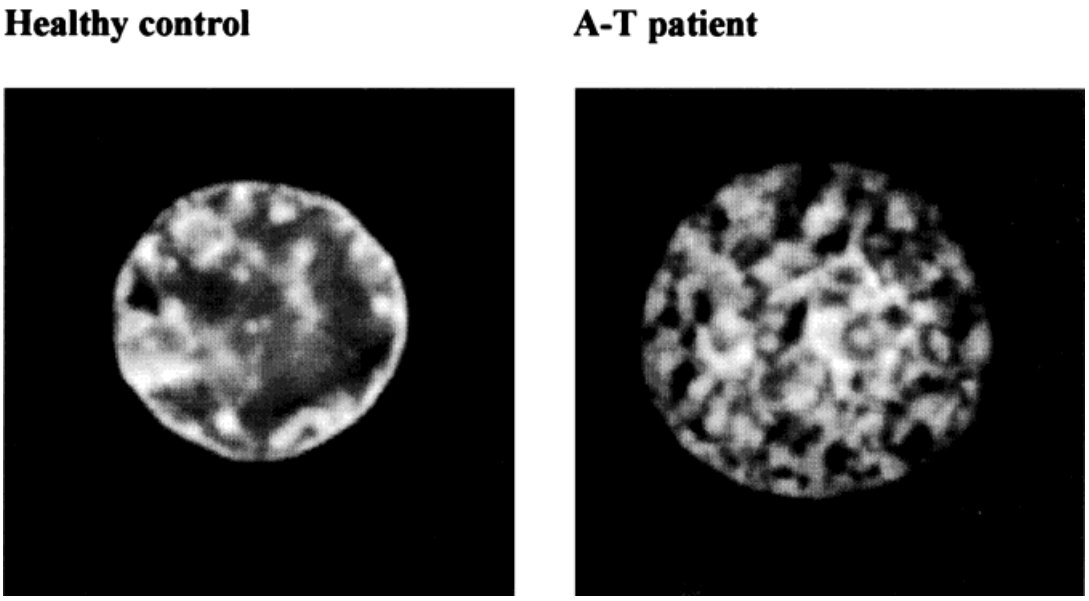

Fig. 2. Equatorial planes of two representative nuclei of the cells under analysis: cell isolated from the A-T patient (cell line AT44RM) and control cell line (cell line 243RM) isolated from the healthy relative. The images have been corrected for the out-of-focus contributions, filtered by using constrained deconvolution, and normalized for the exposure time as described in Materials and Methods.

TABLE II. Integrated Fluorescence Intensity and Nuclear Diameter for Nuclei Isolated From Cultured Lymphoblasts of One A-T Patient (Cell Line AT44RM) and His Healthy Relative (Cell Line 243RM)*

Lymphoblasts	Integrated fluorescence intensity (*10^6)	Nuclear diameter (μm)	Nuclear area (μm^2)	Fluorescence intensity/area
Healthy control	3.0 ± 1	4.4 ± 0.7	15.2 ± 2.5	0.19 ± 0.6
A-T patient	3.8 ± 1	5.9 ± 1.1	27.3 ± 4.1	0.13 ± 0.4

*The intensitometric and morphological parameters have been evaluated on nuclear images acquired at low magnification (40× objective). The standard deviations are also reported for each value.

cessed image. Both the histograms (Fig. 3) show a multimodal distribution of the fluorescence intensity due to the presence of differently condensed chromatin fibers [Mascetti et al., 1996; Nicolini et al., 1997]. A quantitative analysis of the histograms has been made by using a Gaussian decomposition method [Bartel et al., 1979] which allows us to extract the componing peaks. Three main peaks have been individuated in each average histogram and the two nuclear images have been segmented by using the corresponding intensity ranges. In Figure 4 we can see for each nucleus the domains at low (200–700 a.u.), middle (700–1,200 a.u.), and high (1,200–1,700 a.u.) intensity obtained by the segmentation. Each of these levels can be related to differently condensed chromatin structures. A different localization of these structures is evident when the nuclei from the A-T patient and the control are compared: In particular we can see that in A-T nuclei the chromatin domains at high intensity occupy a reduced percentage area of the entire nucleus in comparison to the control. They are also localized preferentially at the center of the nucleus rather than at the periphery as in the control. These high intensity domains should correspond to highly condensed chromatin regions [Mascetti et al., submitted] that therefore are reduced in the A-T nuclei in accordance with the previously discussed data. A different distribution of the domains at low intensity is also evident between the A-T and the control nuclei, with the control showing a less fragmented organiza-

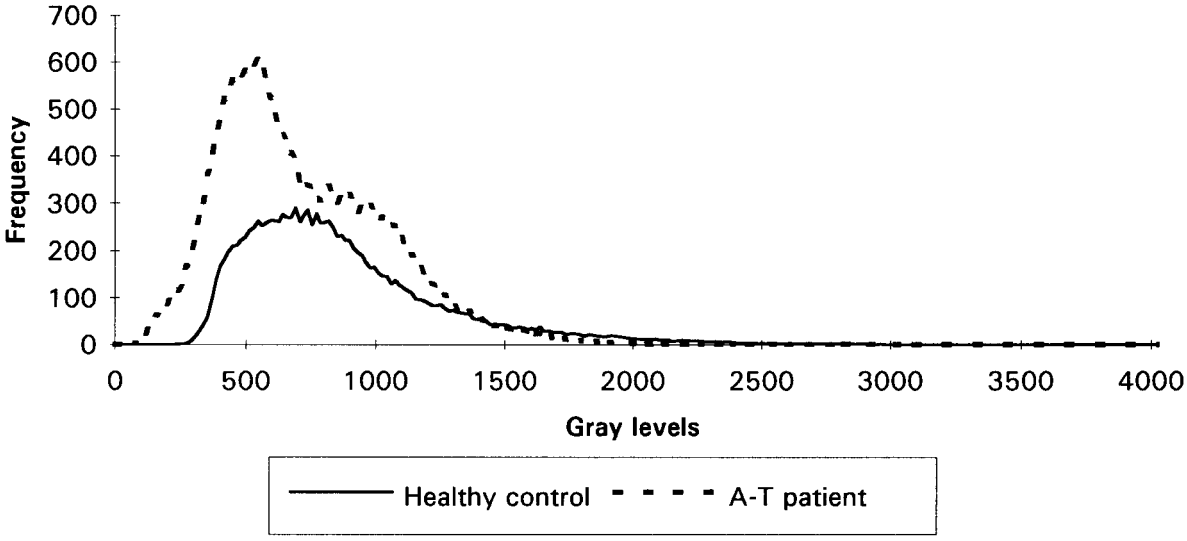

Fig. 3. Average fluorescence histograms reporting the average frequency distribution of the nuclear fluorescence intensity both for cells from the A-T patient (cell line AT44RM) and the healthy relative (cell line 243RM).

tion of this domain associated with less condensed chromatin. These differences of chromatin organization are not related to different cell cycle phases because the cells have been synchronized at G1/S phase by incubation with hydroxyurea before the experiments. It is interesting to note that the interphase nucleus is an inhomegeneous and compartmentalized structure with specific functions localized at specific chromatin domains [for a review see van Driel et al., 1995]. These domains probably are nonrandomly organized within the nucleus, but at the moment we do not understand the relationship between folding—nuclear localization—transcriptional activity at the level of a chromosome domain.

Finally we calculated, starting from the histograms of both samples, the three morphometric parameters chosen to quantitatively describe the nuclear chromatin (Table III). In comparison with the healthy family member the nuclei of the A-T patient show a decrease of both "Heterogeneity" (from 0.81 to 0.73) and "Condensation" (from 0.68 to 0.62) parameters that suggest a chromatin decondensation as a consequence of the disease. At the same time A-T nuclei show an increase of the "Clump" (from 0.83 to 0.85). This result means that nuclei of the A-T patient exhibit an increase of the size of chromatin domains with respect to the healthy relative.

DISCUSSION

Recent studies showed that the normal copy of the ATM gene encodes a protein similar to the phosphatidylinositol 3-kinase (PI 3-kinase), an enzyme involved in the transfer of signals, the prevention of apoptosis, and the control of the cell cycle. Despite these homologies, the function of the ATM gene product remains unknown.

Normal ATM protein probably plays a role in arresting cell cycle advance following genome damage stemming from events such as exposure to ionizing radiation. Most of the mutations analyzed for A-T patients should lead to a premature truncation of the protein product with a supposed damage to the protein function.

The A-T patient of our study shows a marked deletion (201 bp) in ATM gene which is probably associated with a reduced activity of this protein [Savitsky et al., 1995].

In spite of the progress made in the last few years, the pleiotropic nature of the A-T phenotype does not appear to be completely explained by mutations in the ATM gene. Our starting hypothesis was that wider modifications of chromatin higher-order structure and distribution could be associated with this syndrome. The results of our approach corroborate this hypothesis. In fact our data point to a decondensation

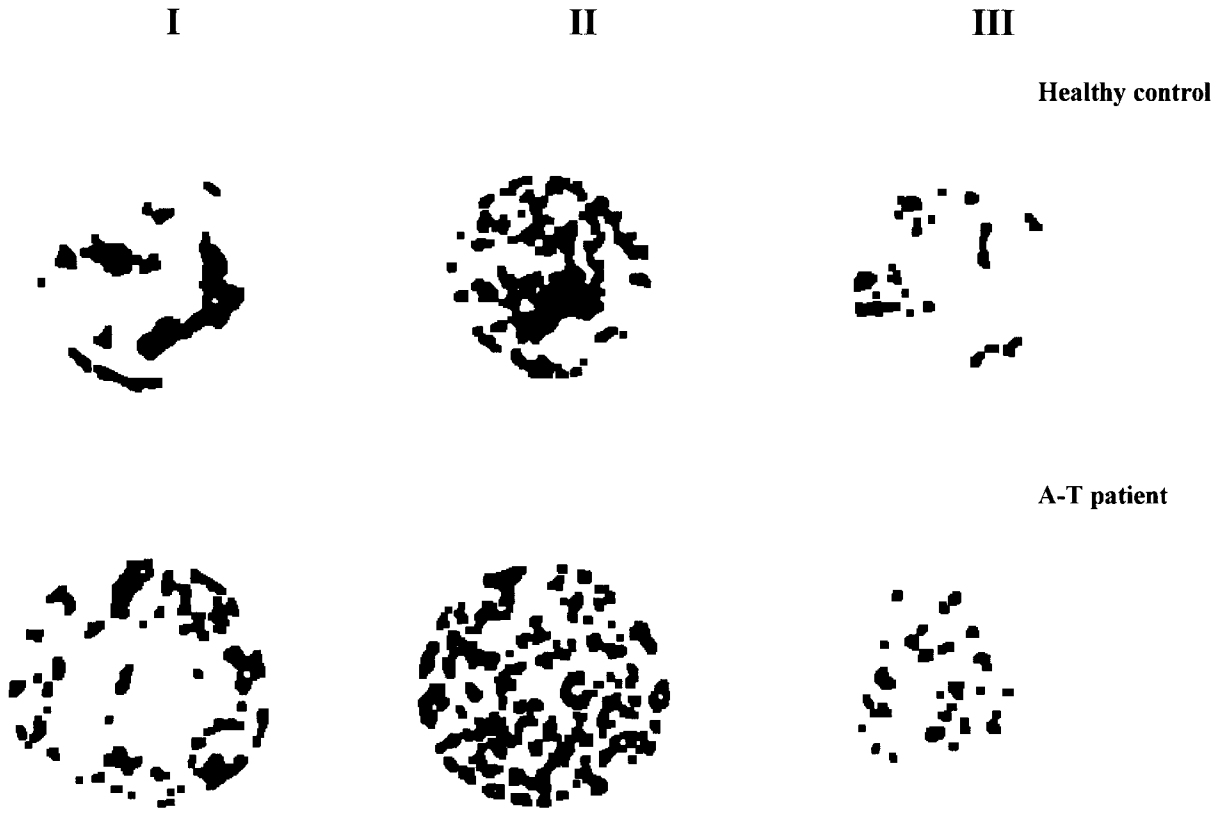

Fig. 4. Distribution of the chromatin domains exhibiting different ranges of fluorescence intensity: I (low: 200–700 a.u.), II (middle: 700–1,200 a.u.), III (high: 1,200–1,700 a.u.) for the same two nuclei reported in Figure 2. The domains have been obtained by the image segmentation using the values provided by the guassian decomposition of the histograms.

TABLE III. Three Different Parameters Related to the Chromatin Distribution and Organization Inside the Nucleus Measured for Nuclei Isolated From Cultured Lymphoblasts of One A-T Patient (Cell Line AT44RM) and His Healthy Relative (Cell Line 243RM)*

Lymphoblasts	Hetero-geneity	Clump	Conden-sation
Healthy control	0.81 ± 0.07	0.83 ± 0.02	0.68 ± 0.06
A-T patient	0.73 ± 0.08	0.85 ± 0.04	0.62 ± 0.05

*The morphometric parameters have been estimated on nuclear images acquired at higher magnification (100× objective).

of the nuclear chromatin as a consequence of the ATM mutation in the case of the analyzed patient. The chromatin decondensation is observed both at the level of nucleosome (an unfolding of core DNA towards linker DNA) and at the level of highly folded chromatin (an unfolding of the highly condensed fiber towards a partially folded one).

In accordance with common opinion, this observed decondensation should be associated with a higher transcriptional and replicative activity of cells with this ATM mutation (a rather large deletion in this case) in comparison with the healthy family member.

It is interesting that differences of chromatin condensation have already been reported between transformed and control cells and that transformed cells have fewer heterochromatin domains in comparison with untransformed ones [Barboro et al., 1993]. In accordance with these data, A-T patients usually exhibit an increased predisposition to cancer (particularly to leukemias and lymphomas).

A further examination of this topic will concern the analysis of more than one A-T patient in order to evaluate how the changes of chromatin structure and distribution may be related

with the seriousness of the disease and with the kind of ATM defect (deletion vs. puntiform mutation, width of deletion, etc.).

ACKNOWLEDGMENTS

We would like to extend our gratitude to Mr. Fabrizio Nozza and Cristina Rando for their expert technical collaboration.

REFERENCES

Agard DA. 1984. Optical sectionning microscopy: cellular architecture in 3 dimensions. Annu Rev Biophys Bioeng 13:191–219.

Agard DA, Hiraoka Y, Shaw P, Sedat J. 1989. Fluorescence microscopy in three-dimensions. Meth Cell Biol 13:191–219.

Allera C, Lazzarini G, Patrone E, ALberti I, Barboro, Sanna P, Melchiori A, Parodi S, Balbi C. 1997. The condensation of chromatin in apoptotic thymocytes shows a specific structural change. J Biol Chem 272:16:10817–10822

Barboro P, Pasini A, Parodi S, Balbi C, Cavazza B, Allera C, Lazzarini G, Patrone E. 1993. Chromatin changes in cell transformation: a differential scnning calorimetry study. Biophys J 1690–1699.

Bartels PH. 1979. Numerical evaluation of cytological data: Description of profiles. Anal Quant Cytol Histol 1:20–28.

Belmont A, Bruce K. 1994. Visualization of G1 chromosomes: a folded, twisted, supercoilde chromonema model of interphase chromatid structure. J Cell Biol 127:2: 287–302.

Bishop DT, Hopper J. 1997. AT-tributable risk. Nat Genet 15:226.

Brown KD, Ziv Y, Sadanandan SN, Chessa L, Collins F, Shiloh Y, Tagle D. 1997. The AT gene product, a constitutively expressed nuclear protein that is not up-regulated following genome damage. Proc Natl Acad Sci USA 94: 1840–1845.

Chessa A, Lisa O, Fiorani G Zei. 1994. Ataxia Telangiectasia in Italy: genetic analysis. Int J Rad Biol 66:S31–S33.

Cremer T, Kurtz A, Zirbel RM, Dietzel S, Rinke B, Schrock E, Speicher MR, Mathieu U, Jauch A, Emmerich P, Shertan H, Ried T, Cremer C, Lichter P. 1993. Role of chromosome territories in the functional compartmentalization of the cell nucleus. Cold Spring Harbor Symp Quant Biol 58:777–792.

Eilis R, Dietzel S, Bertin E, Granzow M, Schrock E, Speicher MR, Volm T, Ried T, Robert-Nicoud M, Cremer C, Cremer T. 1996. Three-dimensional reconstruction of painted human interphase nuclei: active and inactive X chromosome territories have similar volume but differ in shape and surface structure. J Cell Biol 135:1427–1440.

FitzGerald M, Bean J, Hedge S, Unsal H, MacDonald D, Harkin D, Finkelsein D, Isselbacher K, Haber D. 1997. Heterozygous ATM mutations do not contribute to early onset of breast cancer. Nat Genet 15:307–310.

Frenster JH. 1974. The cell nucleus, Bush H, editor. New York and London: Academic Press. pp 565–580.

Gavazzo P, Vergani L, Mascetti G, Nicolini C. 1997. Effects of Histone acetylations on higher order chromatin structure and function. J Cell Biochem 64:3:466–475.

Gilad R, Khosravi R, Harnik R, Ziv Y, Shkedy D, Galanty Y, Frydman M, Levi J, Sanal O, Chessa L, Smeets D, Shiloh Y, Bar-Shira A. 1998. Identification of ATM mutations using extended RT-PCR and restriction endonuclease fingerprinting, and elucidation of the repertoire of A-T mutations in Israel. Hum Mutation 11:69–75.

Haussinger D. 1996. The role of cellular hydration in the regulation of cell function. Biochem J 313:697–710.

Hiraoka Y, Sedat JW, Agard DA. 1987. The use of CCD camera for quantitative optical microscopy of biological structures. Science 238:36–41.

Hutchison N, Weintraub H. 1985. Localization of DNase I sensitive sequences to specific regions of interphase nuclei. Cell 43:471–482.

Kurtz A, Lampel S, Nickolenko JE, Bradl J, Benner A, Zirbel RM, Cremer T, Lichter P. 1996. Active and inactive genes localize preferentially in the periphery of chromosome territories. J Cell Biol 135:1195–1202.

Lamond AI, Earnshaw W. 1998. Structure and function in the nucleus. Science 280:548–553.

Lavin M, Shiloh Y. 1997. The genetic defect in Ataxia Telangiectasia. Annu Rev Immunol 15:177–202.

Lewin B. 1994. Chromatin and gene expression: constant questions but changing answers. Cell 79:397–406.

Mascetti G, Vergani L, Diaspro A, Carrara S, Nicolini C. 1996. Effects of fixatives on calf thymocytes chromatin: 3D High Resolution Fluorescence Microscopy. Cytometry 23:2:110–125.

Myc A, Traganos F, Lara J, Melamed MR, Darzynkiewicz Z. 1992. DNA stainability in aneupolida breast cancer tumors: comparison of four DNA fluorochromes differing in binding properties. Cytometry 13:389–394.

Nicolini C. 1997. Genome Structure and function NATO ASI Series, 3.

Nicolini C, Carrara S, Mascetti G. 1997. High order DNA structure as inferred by optical fluorimetry and scanning calorimetry. Mol Biol Rep 24:235– 246.

Nicolini C, Diaspro A, Vergani L, Cittadini G. 1988. In situ thermodynamic characterization of chromatin and of other cell macromolecules during cell cycle. Int J Biol Macrom 10:137–144.

Nicolini C, Trefiletti V, Cavazza B, Cuniberti C, Patrone E, Carlo P, Brambilla G. 1983. Quaternary and quinternary structure of chromatin from resting cells: high resolution computer analysis of liver nuclei and differential scanning calorimetry. Science 219:176.

Russo I, Barboro P, Alberti I, Parodi S, Balbi C, Allera C, Lazzarini G, Patrone E. 1995. Role of H1 in chromatin folding: a thermodynamic study of chromatin reconstitution by DSC. Biochemistry 34:301–311.

Savitsky K, Bar Shira, Gilad S. 1995. A single Ataxia Telangiectasia gene with a product similar to PI-3 Kinase. Science 268:1749–1753.

Savitsky K, Sfez S, Tegle D, Ziv Y, Sartiel A, Collins F, Shiloh Y, Rotman G. 1995. The complete sequence of the coding region of the ATM gene reveals similarity to cell cycle regulators in different species. Hum Mol Genet 4:2025–2032.

Touchette NA, Cole RD. 1985. Differential scanning calorimetry of nuclei reveals the loss of major structural features in chromatin by brief nuclease treatment. Proc Natl Acad Sci USA 82:2642–2645.

van Driel R, Wansink DG, van Steensel B, Grande MA, Schul W, de Jong L. 1995. Nuclear domains and nuclear matrix. Int Rev Cytol 162A:151–189.

van Holde KE. 1989. Chromatin structure. New York: Springer Verlag.

Vergani L, Gavazzo P, Facci P, Diaspro A, Mascetti G, Arena N, Gaspa L, Nicolini C. 1992. Fluorescence cytometry of microtubules and nuclear DNA during cell-cycle and reverse transformation. J Cell Biochem 50:201–209.

Vergani L, Gavazzo P, Mascetti G, Nicolini C. 1997. Ethidium Bromide intercalation and chromatin structure: a thermal analysis. Termochimica Acta 294:193–204.

Vergani L, Mascetti G, Nicolini C. 1998. Effects of polyamines on higher-order folding of in situ chromatin. Mol Biol Rep 25:4:237–244.

Wolffe A. 1994. Chromatin structure and function. London: Academic Press.

Young IT, Verbeek PW, Mayall BH. 1986. Characterization of chromatin distribution in the cell nucleus. Cytometry 7:467–474.

Zink D, Cremer T, Saffrich R. 1998. Structure and dynamics of human chromosome territories in vivo. Hum Genet 102:241–251.